

Low computational cost matching pursuit algorithm for LCX-based Intruder Detection System

Tomonori Sato¹, Ziji Ma², Takeshi Higashino³, and Minoru Okada⁴, Non-members

ABSTRACT

The leaky coaxial cable (LCX) based intruder detection system detects intruders by making efficient use of time-variation of the channel impulse response among the cables. Recently, a compressed sensing (CS)-assisted intruder detection system has been proposed for improving the accuracy of the intruder detection. Although the CS-assisted system can improve the false detection probability performance efficiently, it is difficult to implement it because of its huge computational cost requirement. This paper proposes a modified matching pursuit (MMP) algorithm for reducing the computational cost of the CS-assisted intruder detection scheme. MMP can reduce the computational cost by limiting the search range in the vicinity of impulse response peaks estimated at the last measurement. Computer simulation results show the proposed system can reduce the computational cost for the conventional CS-based algorithm without degradation in the false detection performance.

Keywords: LCX, Compressed Sensing, Matching Pursuit, Low Complexity Algorithm

1. INTRODUCTION

There has been a great demand for intruder detection systems for managing the securities of the key facilities such as the airports, rail tracks, military bases, nuclear power plants, schools, and so on. Many kinds of sensor devices, including infrared sensors, cameras and microwave radars, etc. are widely used for intruder detection. However, these sensors are not suitable for wide area surveillance because of limitation in the sensing range. To realize reliable intruder detection in wide areas, LCX-based intruder detection systems have been studied[1-3].

A typical LCX-based intruder detection system is composed of a pair of LCX cables and an impulse response measuring equipment. The wide-band RF

(Radio Frequency) signal is transmitted through either one of the LCX cables. The signal is received by the other side of the cables. The signal is propagated among a pair of LCX cables. The received signal is applied to the impulse response estimator, where the cross-correlation between the transmitted and received signals is calculated to derive the impulse response of the propagation channel. When an intruder enters the region between the two cables, the intruder scatters the transmitted signal, and it induces a change in the impulse response. We can detect the intruder by this variation in the impulse response.

The LCX-based intruder detection system has several advantages over the conventional intruder detection systems. The LCX-based intruder detection system allows us to detect the intruders in a narrow and long range even with hundreds of meters. Furthermore, it can localize the position of intruders along the LCX cables.

Although the LCX based detection system has the attractive advantages, it has problems in the accuracy of the intruder detection. Especially, the false alarm rate becomes unacceptably high when the disturbances such as the vibration of the LCX cables occurs. Since the LCX-based intruder detection system detects an intruder by sensing the time variation of the channel impulse response, the vibration of LCX cables could induce a false alarm. Therefore a new detection algorithm is required to solve this problem.

The conventional schemes employ the Least Square (LS) algorithm to estimate the impulse response. For the LS method, additive noise gives considerable effect on the received signal, so it is difficult to improve false error rate performance. To solve the problem, we have proposed a detection method based on Compressed Sensing (CS) algorithm[4]. CS method can estimate the impulse response vector accurately in a noisy environment, only if the vector is sparse.

However, the proposed CS-based intruder detection system requires huge computational cost because it repeatedly performs large size matrix calculations. To reduce the computational cost, we propose a modified matching pursuit algorithm that can largely decrease the computational complexity for solving CS. Since the motion of the targets is relatively slow comparing with the measuring interval, the difference in target positions between the current and last estima-

Manuscript received on December 15, 2012 ; revised on May 29, 2014.

Final manuscript received on October 17, 2016.

^{1,2,3,4} The authors were with Graduate School of Information Science, Nara Institute of Science and Technology (NAIST), Ikoma-shi, 630-0192 Japan, E-mail: tomonori-sa@is.naist.jp, ziji-ma@hnu.edu.cn, higa@is.naist.jp and mokada@is.naist.jp

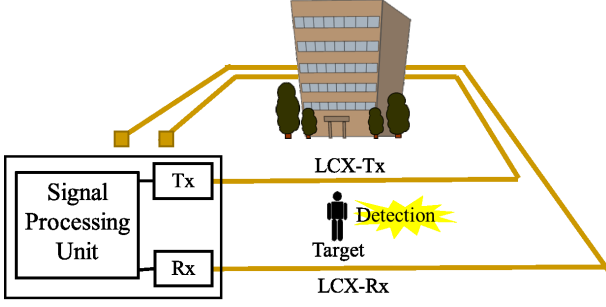


Fig. 1: the structure of LCX-based intruder detection system

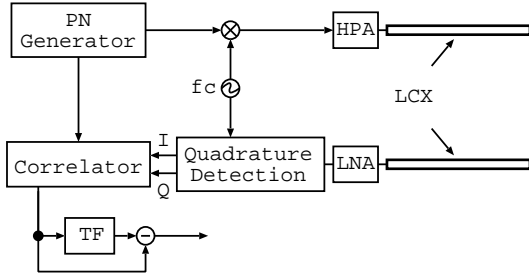


Fig. 2: System Model

tion period is small. Firstly, the system estimates the largest positions using the conventional CS algorithm. After that, the search for matching pursuit is conducted only around the vicinity of the target positions estimated at the previous estimation. The search is repeatedly performed at the each estimation period. In this algorithm, we can reduce the computational cost thanks to the limited search range. Computer simulation result shows that our method can reduce the processing time for estimating the target positions.

2. INTRUDER DETECTION SYSTEM USING LCX

2.1 System Model

Figure 1 illustrates the overview of intruder detection system using LCX cables. In the system, a pair of LCX cables is implemented around vital areas as shown in Fig. 1. The sounding signal is transmitted from the transmitter-side LCX cable(LCX-Tx). The transmitted signal is received by the receiver-side cable(LCX-Rx). When an intruder enters the area between two cables, the sounding signal is scattered by the intruder. The signal processing unit measures the impulse response by calculating the cross-correlation between transmitted and received signals. We can detect the intruder by observing the change in the impulse response.

The block diagram of the transmitter and receiver are shown in Figure 2. The RF (Radio Frequency) carrier signal of the frequency, f_c , is modulated by

the PN (Pseudo-random Noise) code generated by the PN generator. The modulated signal is amplified by the high power amplifier (HPA) and applied the transmitter-side LCX cable. The receiver(Rx) is connected to receiver-side LCX cable. The received signal is first amplified by the low noise amplifier (LNA) and then applied to the quadrature detector for frequency down-conversion. The channel impulse response is estimated by calculating the cross-correlation among the frequency down-converted received signal and the PN code. The estimated channel impulse response is stored in the time-frame memory (TF). Finally, the time-variation in the estimated channel impulse response is calculated by subtracting the stored response from the current one. We can detect the obstacles between LCX cables by observing the time-variation [5].

Let us go into the further details of the detection system. The transmitted signal in equivalent low-pass expression[6] $x(t)$ is given by

$$x(t) = \sum_{k=0}^{N-1} x_k f(t - kT_c), \quad (1)$$

where $x_k \in \pm 1$ is a PN sequence of length, N , T_c is the chip duration, and

$$f(t) = \begin{cases} \frac{1}{\sqrt{T_c}} & |t| \leq \frac{T_c}{2} \\ 0 & \text{otherwise} \end{cases} \quad (2)$$

is the pulse waveform.

The generated signal, $x(t)$, is frequency up-converted, amplified and emitted from the transmitter-side LCX cable. The transmitted signal propagates through the gap between the transmitter and receiver-side LCX cables. The Received signal from the receiver-side LCX cable is amplified, and frequency down-converted. The received signal in the equivalent low-pass expression is given by

$$y(t) = \int_{\tau=0}^{\infty} g(\tau; t) x(t - \tau) d\tau + z(t), \quad (3)$$

where $g(\tau; t)$ is an channel impulse response, and $z(t)$ is an Additive White Gaussian Noise (AWGN) component.

The channel impulse response can be divided into two components, namely,

$$g(\tau; t) = g^{normal}(\tau) + g^{scat}(\tau; t), \quad (4)$$

where $g^{normal}(\tau)$ and $g^{scat}(\tau; t)$ are the direct paths and the scattered signal components, respectively. The direct path component is considered as the impulse response when no obstacles between the paired

LCX cables exist. Therefore, $g^{normal}(\tau)$ is given by

$$g^{normal}(\tau) = \sum_{m=0}^{N_{txslot}} \sum_{n=0}^{N_{rxslot}} a_{m,n} \delta(\tau - \tau_{m,n}) e^{-j\theta_{m,n}}, \quad (5)$$

where N_{txslot} and N_{rxslot} are the numbers of slot in transmitter and receiver LCXs respectively. Also, $a_{m,n}$ and $\tau_{m,n}$ denote the amplitude and delay time among the m -th slot of the transmitter-side LCX n -th slot of the receiver-side one.

The impulse response corresponding to scattered signal component is given by

$$g^{scat}(\tau; t) = \sum_{m=0}^{N_{txslot}} \sum_{n=0}^{N_{rxslot}} \frac{\lambda^2 \sigma_0}{(4\pi)^3 d_1^2 d_2^2} \delta(\tau - \tau'_{m,n}) e^{-j(\theta'_{m,n} + 2\pi f_{obst} t)}, \quad (6)$$

where λ is the free-space wavelength. d_1 and d_2 are the distance between transmitter-side cable and the obstacle, and the distance between the obstacle and the receiver-side cable, respectively. f_{obst} is the Doppler frequency caused by the motion of the obstacle, and σ_0 is the effective cross-section due to the scattering obstacle.

The cross correlation between $y(t)$ and $x(t)$ is given by

$$R(\xi) = \int_0^{NT_c} y(t + \xi) x^*(t) dt. \quad (7)$$

Substituting Eq (3) into Eq (7), we can rewrite the correlation function as:

$$R(\xi) = \int_0^\infty \int_0^{NT_c} g(\tau; t) x(t + \xi - \tau) x^*(t) dt d\tau. \quad (8)$$

Let us assume that $g(\tau; t)$ is time-invariant between $t = 0$ and $t = NT_c$, or the time variation in the channel impulse response can be neglected during the PN code duration. This implies that $g(\tau; t)$ is approximately written as:

$$g(\tau; t) = \tilde{g}(\tau). \quad (9)$$

Therefore, Eq (8) is now given by

$$R(\xi) = \int_0^\infty \tilde{g}(\tau) \int_0^{NT_c} x(t + \xi - \tau) x^*(t) dt d\tau. \quad (10)$$

According to the auto-correlation property of the PN code, the correlation function of the transmitted signal is derived as

$$\int_0^{NT_c} x(t) x^*(t - \tau) dt = \begin{cases} N & (\tau = 0) \\ \cong 0 & (\tau \neq 0) \end{cases}. \quad (11)$$

Substituting Eq (11) into Eq (10), we can obtain

the channel impulse responses corresponding as:

$$R(\xi) = Ng(\tau) |_{\xi=\tau}. \quad (12)$$

The scattered signal component caused by an obstacle between the paired LCX cables, $g^{scat}(\tau)$, can be obtained by $g^{obst}(\tau) - g^{normal}(\tau)$ and finally the location of the intruding obstacle can be estimated.

2.2 Least Square Method

Let us define the vector form representation of the received signal as: $\mathbf{y} = [y_0, y_1, \dots, y_{M-1}]^T$, where $y_k = y(kT_c)$ and $M = 2N - 1$. Then, Eq (3) can be expressed as [7]

$$\mathbf{y} = \mathbf{X}\mathbf{g} + \mathbf{z}, \quad (13)$$

where

$$\mathbf{X} = \begin{bmatrix} x_0 & 0 & \cdots & 0 \\ x_1 & x_0 & \cdots & 0 \\ \vdots & x_1 & \ddots & 0 \\ x_{N-1} & \vdots & \ddots & x_0 \\ 0 & x_{N-1} & \ddots & x_1 \\ \vdots & \vdots & \ddots & \vdots \\ 0 & 0 & \cdots & x_{N-1} \end{bmatrix} \quad (14)$$

is the convolution matrix, and $\mathbf{z} = [z_0, z_1, \dots, z_{M-1}]$ is the AWGN vector.

According to Eq (11), the matrix \mathbf{X} satisfies the following relationship:

$$\mathbf{X}^H \mathbf{X} = N\mathbf{I}_N, \quad (15)$$

where \mathbf{I}_N is the $N \times N$ identity matrix. The channel impulse response vector, \mathbf{g} , is given by

$$\mathbf{g}^{LS} = \arg \min_{\mathbf{g}} \|\mathbf{y} - \mathbf{X}\mathbf{g}\|_2, \quad (16)$$

where $\|\mathbf{a}\|_2 = \sqrt{\sum |a_i|^2}$ is the l_2 norm of \mathbf{a} , and $\arg \min_{\mathbf{x}} f(\mathbf{x})$ gives \mathbf{x}_0 which minimizes $f(\mathbf{x})$.

Therefore, impulse response vector \mathbf{g}^{LS} is represented by following equation.

$$\mathbf{g}^{LS} = (\mathbf{X}^H \mathbf{X})^{-1} \mathbf{X}^H \mathbf{y}. \quad (17)$$

According to Eq (15), we can get

$$\mathbf{g}^{LS} = \mathbf{X}^H \mathbf{y}. \quad (18)$$

2.3 Compressed Sensing Method

If the unknown vector is sparse, we can estimate the vector by making efficient use of compressed sensing (CS) method[8][9]. In the LCX based intruder detection system, the impulse response corresponding to the scattered signal has non-zero value only at the location where the intruder exists. Therefore,

the impulse response vector is sparse. We can apply CS to the channel response estimation of the intruder detection system.

Now, let us define that the impulse response vector corresponding to the scattered signal is \mathbf{g}^{CS} . Then, CS is formulated as [10, 11]:

$$\begin{aligned} \mathbf{g}^{CS} &= \arg \min_{\tilde{\mathbf{g}}} \|\tilde{\mathbf{g}}\|_1 \\ \text{s.t.} \quad &\|\mathbf{X}^H(\mathbf{y} - \mathbf{X}\tilde{\mathbf{g}})\|_1 \leq \lambda_c \end{aligned} \quad (19)$$

where $\|\mathbf{a}\|_1 = \sum_i |a_i|$ is the l_1 norm of \mathbf{a} , and

$$\lambda_c = \sqrt{2N\sigma(1+a)\log N} \quad (20)$$

is the noise margin, where σ is the standard deviation of the noise, and $a \geq 0$ is the relaxation factor. Eq. (20) can be solved by using the linear programming. However CS using the linear programming requires huge computational cost. Therefore, in the following, we propose an another algorithm for solving CS.

3. COMPUTATIONAL COST USING MODIFIED MATCHING PURSUIT

As we mentioned in the previous section, CS-based channel impulse response estimation requires huge computational cost. To reduce the computational cost, we propose a modification of matching pursuit algorithm. In the following, we will briefly explain the principle of Matching Pursuit[12]. Then we propose a modified algorithm for reducing the cost.

3.1 Matching Pursuit

Suppose that \mathbf{g}^{mp} is an arbitrary m -sparse signal. The M -dimensional observe signal vector \mathbf{y} is given by

$$\mathbf{y} = \mathbf{X}\mathbf{g}^{mp}, \quad (21)$$

where $M \times N$ matrix \mathbf{X} whose rows are the measurement vectors. We refer to \mathbf{X} as the measurement matrix and denote its columns by $[\mathbf{x}_0, \dots, \mathbf{x}_{N-1}]$.

To identify the ideal signal \mathbf{g}^{mp} , we need to determine which columns of \mathbf{X} participate in the measurement vector \mathbf{y} . The idea behind the algorithm is to pick columns in a greedy fashion. At each iteration, we choose the column of \mathbf{X} that is most strongly correlated with the remaining part of \mathbf{y} . Then we subtract off its contribution to \mathbf{s} and iterate on the residual. One hopes that, after m iterations, the algorithm will have identified the correct set of columns.

The procedure of the recovering signals is represented by the following steps.

1. Initialize the residual $\mathbf{r}_0 = \mathbf{y}$, the index set $\Lambda_0 = \emptyset$, and the iteration counter $i = 1$.
2. Find the index λ_i that solves the easy optimization

problem

$$\lambda_i(t) = \arg \max_{k=0, \dots, N-1} |\langle \mathbf{r}_{i-1}, \mathbf{x}_k \rangle|. \quad (22)$$

3. Augment the index set and the matrix of chosen atoms: $\Lambda_i = \Lambda_{i-1} \cup \{\lambda_i\}$ and $\mathbf{X}_i = [\mathbf{X}_{i-1} \mathbf{x}_{\lambda_i}]$. We use the convention that \mathbf{X}_0 is empty matrix.
4. Solve a least square problem to obtain a new signal estimate:

$$\mathbf{g}_i = \arg \min_{\mathbf{g}} \|\mathbf{y} - \mathbf{X}_i \mathbf{g}\|_2. \quad (23)$$

5. Calculate the new approximation of the data and the new residual

$$\mathbf{r}_i = \mathbf{y} - \mathbf{X}_i \mathbf{g}_i. \quad (24)$$

6. Increment i , and return to Step 2 if $i < m$ or average power of $\|\mathbf{r}_i\|_2 > \eta_r$, where η_r is threshold.
7. The estimate \mathbf{g}^{mp} for the ideal signal has nonzero indices at the components listed in Λ_m . The value of the estimate \mathbf{g}^{mp} in component λ_k equals the k th component of \mathbf{g}_i .

3.2 Modified Matching Pursuit

Although the matching pursuit algorithm mentioned above is capable of detecting the intruders, it is difficult to carry out the calculation within the practical period due to huge computational cost. To reduce the computational cost, we propose a modified matching pursuit algorithm. The motion of the intruder was relatively slow in compared with the observation interval, NT_c . This implies that the channel impulse response at the current observation interval does not drastically change at the next interval. The proposed modified matching pursuit algorithm makes efficient use of the slow variation of the channel impulse response. In the proposed algorithm, the estimation is once carried out by using the original matching pursuit algorithm. After the first estimation is completed, the algorithm stores the positions where the peak value that is larger than the threshold. In the following estimation, the peak search operation original described in step 2 is carried out only in the areas around the vicinity of the peaks detected in the previous estimation.

3.2.1 Derivation Scheme for Peak Position Vector

Now, we explain the further detail of the proposed algorithm in Figure 3. The proposed intruder detection system obtains the sparse impulse response vector $\mathbf{g}^{CS} = [g_0^{CS}, g_1^{CS}, \dots, g_{N-1}^{CS}]$ using CS process at t . Then, the system keeps the indices of elements whose values are larger than threshold η_p . Let us define the peak position vector at the initial stage as $\mathbf{v}_{init}(t) = [v_0^{init}, v_1^{init}, \dots, v_{N-1}^{init}]$. As shown in the graph on top of Figure fig:mmp, the initial position

vector is given by

$$v_k^{init} = \begin{cases} 1 & |g_k^{CS}| > 0 \\ 0 & |g_k^{CS}| = 0 \end{cases}. \quad (25)$$

We could use the initial position vector as a search region if the peak position would not change. In practice, the position varies depending on the motion of the intruders. Therefore, we need to expand the peak position vector.

At Step 1 of Figure 3, we modify the channel impulse response vector \mathbf{g}^{CS} as follows. The modified channel impulse response is given by

$$g_k'^{CS} = \frac{1}{2}|g_k^{CS}| + \frac{1}{4}|g_{k-1}^{CS}| + \frac{1}{4}|g_{k+1}^{CS}|. \quad (26)$$

Then, as shown in Step 2 of Figure 3, the threshold η_p is given by

$$\eta_p = p \|\mathbf{g}'^{CS}\|_2, \quad (27)$$

where p is a coefficient for determining the threshold. As shown in Step 3, \mathbf{g}''^{CS} is calculated as:

$$g_k''^{CS} = \begin{cases} g_k'^{CS} & |g_k'^{CS}| \geq \eta_p \\ 0 & |g_k'^{CS}| < \eta_p \end{cases}. \quad (28)$$

Finally, the modified peak position vector $\mathbf{v}(t) = [v_0, v_1(t), \dots, v_{N-1}(t)]$ is obtained by the following equation:

$$v_k = \begin{cases} 1 & |g_k''^{CS}| > 0 \\ 0 & |g_k''^{CS}| = 0 \end{cases}. \quad (29)$$

In this method, it is important how to decide the threshold η_p . We discuss it in Section 4.1

3.2.2 Detection Scheme using Modified Matching Pursuit

In this section, we show the algorithm of Modified Matching Pursuit using the peak position vector $\mathbf{v}(t-1)$ at certain time $t-1$. In Step 2 in Section 3.1 the inner product operation is carried out for all N vectors as in Eq. (22). The proposed algorithm calculate the system explores by the following algorithm, the inner product and peak search is carried out only for the positions that the elements of the peak position vector obtained in the previous section are '1.' The peak search procedure is

$$\lambda_i(t) = \arg \max_{\{k|v_k(t-1)=1\}} |\langle \mathbf{r}_{i-1}, \phi_k \rangle|. \quad (30)$$

The intruder could exist where the positions corresponding to the non-zero element in $\mathbf{v}(t-1)$.

The procedures of the proposed modified matching pursuit algorithm are the same as the original matching pursuit algorithm described in 3.1 except for the peak search in Eq.(30). The peak search is repeated

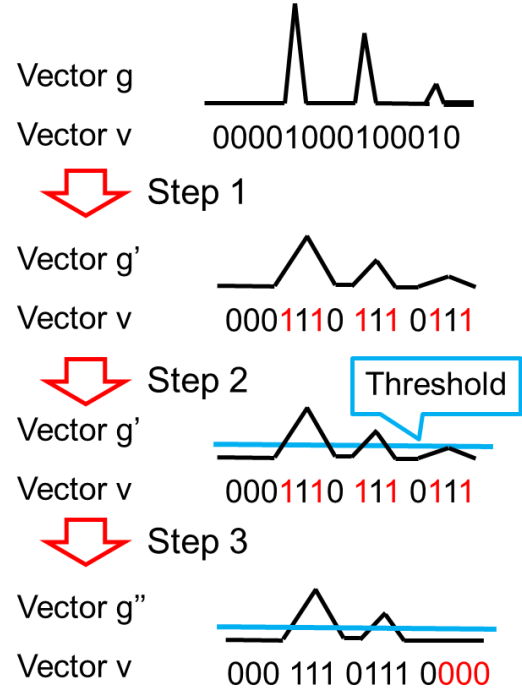


Fig.3: Flow Chart of Modified Matching Pursuit

unless the length of the residual vector is larger than the threshold, η_r^{mmp} .

The threshold is determined by the following procedure. Firstly, we calculate the expected received signal $\|\mathbf{y}_{t-1}^{mmp}\|_2$ when the channel impulse response vector is \mathbf{g}_{t-1}^{CS} . The expected received signal is given by

$$\mathbf{y}_t^{mmp} = \mathbf{X} \mathbf{g}_t^{CS}, \quad (31)$$

We employs

$$\eta_r^{mmp} = \|\mathbf{y}_t - \mathbf{y}_{t-1}^{mmp}\|_2. \quad (32)$$

The number of iteration is at most the number of non-zero elements of $\mathbf{v}(t-1)$. When the l_2 norm the residual vector \mathbf{r}_i is still larger than η_r^{mmp} after the number of iteration reaches the number of non-zero elements, it is probable that the peak arises at a position other than the non-zero positions of $\mathbf{v}(t-1)$. In this case, the original matching pursuit algorithm is carried out for obtaining the proper result.

4. NUMERICAL RESULTS

In this section, we show some numerical results to confirm the performance of the proposed method. Table 1 is the system configuration to run the simulation.

Figure 4 shows a detection area model. We use two 50-meter LCX cables placed in parallel. The transmitter is connected to the upper left endpoint of the LCX cable, and the receiver is connected to the bot-

Table 1: System Configuration

Parameters	Values
LCX length	50 [m]
Width between LCXs	10 [m]
Time symbol(N_t)	32
Frequency	300 [MHz]
bandwidth	60 [MHz]
ε_{lcx}	2.4
PN code size	63
Target speed	1.2[m/s]

Table 2: Computer Simulation Environment

CPU	Intel Core2 Quad Q9650 3.00GHz
RAM	4.00GB
OS	Linux 3.2.0
Programming Language	C++

tom left side.

In the simulation, we assume that one target obstacle exists between two LCX cables and it moves at the speed of 1.2 m/s as in Figure 4.

The simulation is carried out at the simulation environment shown in Table 2. We repeated simulation runs N_t times for evaluating the performance.

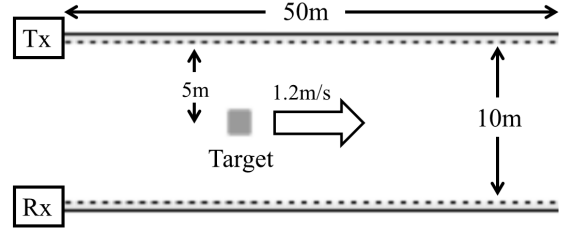
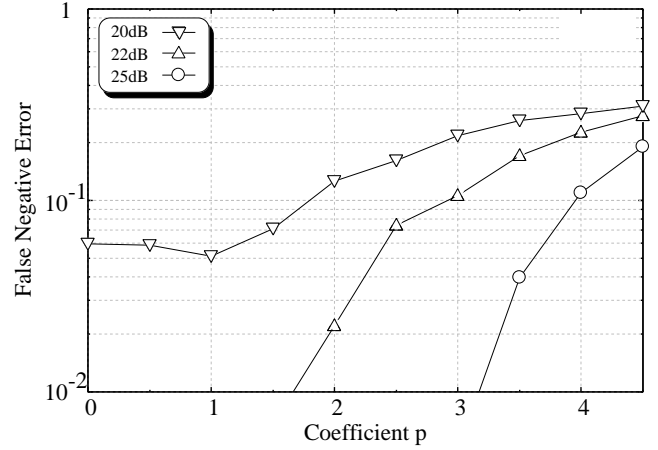
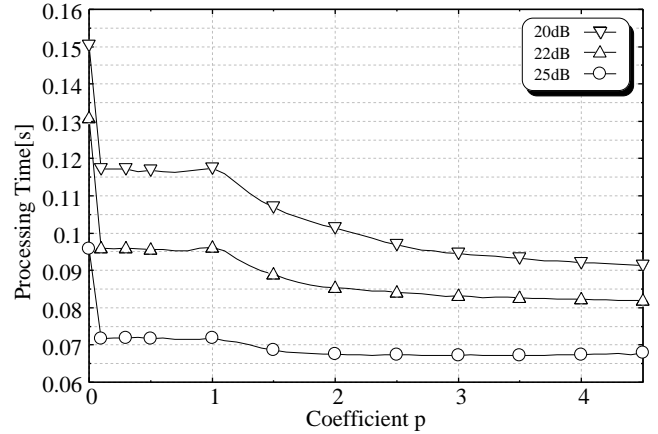
4.1 Verification of coefficient using proposal method

As described in Section 3.2.1, both the false error rate and the processing time vary depending on the peak threshold η_p using Modified Matching Pursuit. Figure 5 and 6 respectively show the false negative error rate and processing time against the coefficient p when CNR is 20dB, 22dB and 25dB, where CNR is the received signal to thermal noise power ratio. Figure 5 shows that the false negative error rate grows with increase in the coefficient and we can get the acceptable false negative error rate if the coefficient p is less than 1. In contrary, the processing time can be reduced with increase in p .

Figure 7 shows the relationship between the false negative error rate and the processing time. The required processing time for obtaining the acceptable error rate performance is about 0.11[s]-0.12[s]. According to Figures 5 and 6, it corresponds that p is around 1. Therefore, we set $p = 1$ in the following analyses.

4.2 Performance evaluations

We evaluate the computational cost of the proposed modified matching pursuit algorithm based intruder detection system. Figure 8 and 9 respectively show iteration count and processing time against CNR using the conventional and the proposed methods. The proposed method can reduce the number of

**Fig.4:** Propagation Area Model**Fig.5:** False negative error rate when coefficient p changes.**Fig.6:** Processing time when coefficient p changes.

iterations by half. Furthermore, the processing time for the proposed method is about 30% of the conventional one.

The false positive rate (FPR) and false negative rate (FNR) performance against CNR are respectively shown in Figure 10 and 11. In Figure 10, the proposed scheme gives lower false positive rate than the conventional one in high CNR region. Also, the proposed scheme can slightly improve the false negative rate performance.

According to these results, we can conclude that

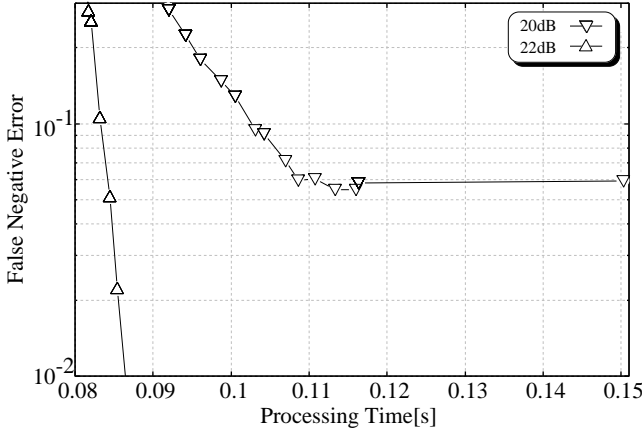


Fig.7: False negative error rate when processing time changes.

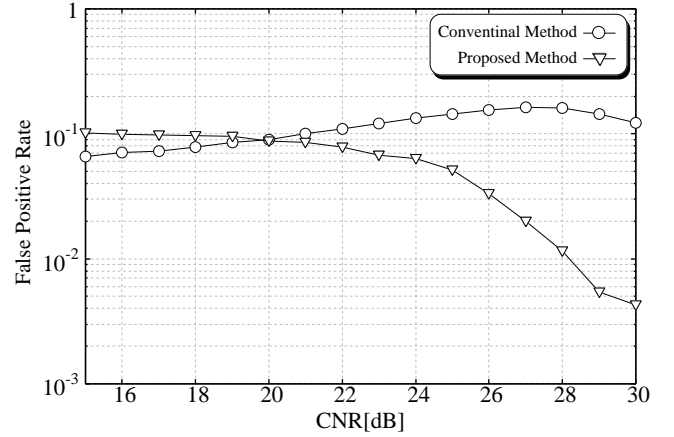


Fig.10: False positive error rate when CNR changes.

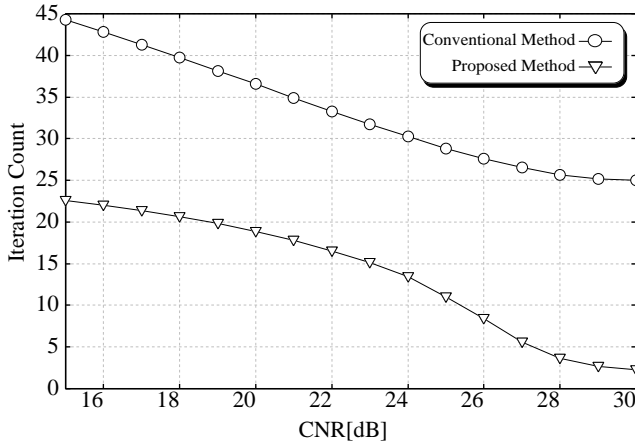


Fig.8: Iteration Count

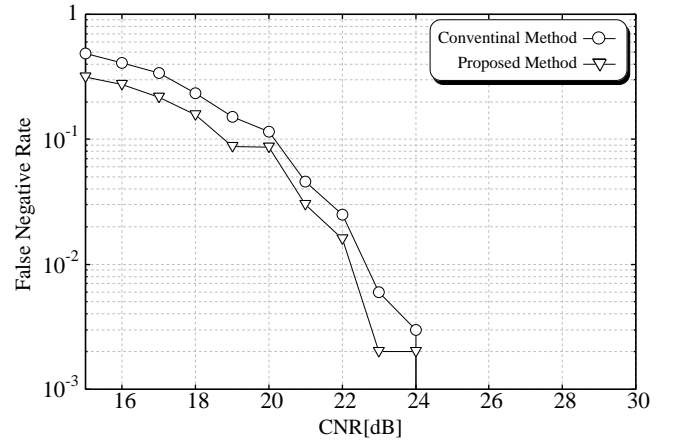


Fig.11: False negative error rate when CNR changes.

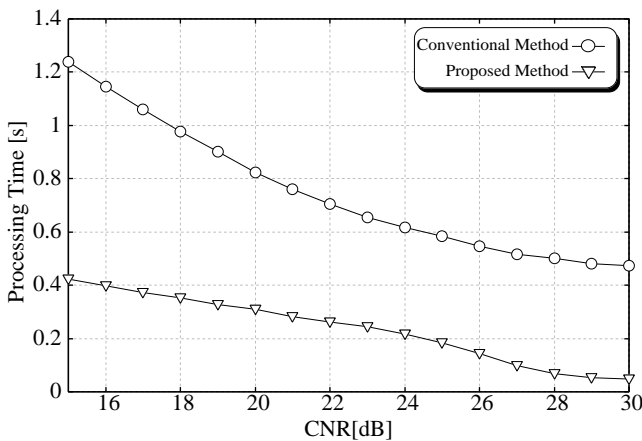


Fig.9: Processing Time

the proposed scheme is capable of reducing the computational cost while maintaining the error rate performance of the conventional CS-based intruder detection algorithm.

5. CONCLUSION

In this paper, we have proposed a reduced complexity intruder detection system based on the modified matching pursuit-based compressed sensing method. We verified the optimal coefficient value of threshold using proposed method and evaluated the iteration count, the procedure time and the false error rate performance by computer simulation.

The optimal coefficient value is 1 in the supposed intruder detection system configuration. The result shows that the proposed method can reduce the computational cost while maintaining the error rate performance.

References

- [1] K. Inomata and T. Hirai, "Microwave back-projection radar for wide-area surveillance system," 34th European Microwave Conference, vol. 3, no. 11, pp. 1425-1428, Oct 2004.
- [2] K. Nishikawa, T. Higashino, K. Tukamoto, and S. Komaki, "TDOA based wireless positioning method using leaky coaxial cable [in japanese],"

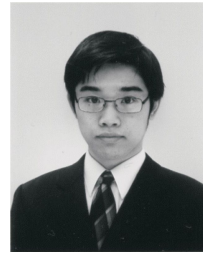
The transactions of the Institute of Electronics, Information and Communication Engineers. B, vol. J92-B, no. 1, pp. 320–327, Jan 2009.

- [3] K. Inomata and T. Hirai, “An analysis of propagation loss characteristics in indoor short range wireless communications using ray-tracing technique [in japanese],” Technical report of IEICE, vol. SANE2005, no. 101, pp. 29–34, Feb 2006.
- [4] T. S. Okada, “A study on detection accuracy for intruder detection system using leaky coaxial cable,” 2012 International Conference on Embedded Systems and Intelligent Technology, pp. 167–170, Jan 2012.
- [5] G. Marubayashi, M. Nakagawa, and R. Kohno, *Spread Spectrum Communication and Its Applications*. The Institute of Electronics, Information and Communication Engineers, 1998.
- [6] S. Stein and J. Jay Jones, *Modern Communication Principles With Application to Digital Signaling*. McGRAW HILL, 1970.
- [7] A. Goldsmith, *Wireless Communications*. New York: Cambridge University Press, 2005.
- [8] D. L. Donoho, “Compressed sensing,” Information Theory, IEEE transaction on, vol. 52, no. 4, pp. 1289–1306, Apr 2006.
- [9] T. Tanaka, “Mathematics of compressed sensing,” IEICE Fundamentals Review, vol. 4, no. 1, pp. 39–47, June 2010.
- [10] W. U. Bajwa, J. Haupt, G. Raz, and R. Nowak, “Compressed channel sensing,” Conf. Information Sciences and Systems, pp. 5–10, Mar 2008.
- [11] W. U. Bajwa, J. Haupt, A. M. Sayeed, and R. Nowak, “Compressed channel sensing: A new approach to estimating sparse multipath channels,” Proceedings of the IEEE, vol. 98, no. 6, pp. 1058–1076, June 2010.
- [12] J. A. C. Gilvert, “Signal recovery from random measurement via orthogonal matching pursuit,” IEEE Transactions on Information Theory, vol. 53, no. 12, pp. 4655–4666, Dec 2007.



measurement systems.

Ziji Ma received the B.E. degree in electronics engineering and the M.S. degree in electronics science and technology from Hunan University, China, in 2001 and 2007, respectively. He received the Ph.D in information systems from Nara Institute of Science and Technology in 2012. Now he is working at Hunan University, China. His major research interests include wireless communications, digital signal processing and



an Associate Professor. From 2014 to 2015, he was a visiting researcher at Georgia Institute of Technology, Atlanta, U.S. His research interest is on radio over fiber technique, wireless communication including OFDM, MIMO, digital broadcasting, wireless position location and wireless power transfer. Dr. Higashino is a member of IEEE and IEICE.

Takeshi Higashino received the B.E., M.E. and Ph.D. degrees in communications engineering from Osaka University, in 2001, 2002 and 2005 respectively. From 2005 to 2012, he was an assistant professor in the Division of Electrical, Electronic and Information Engineering at Osaka University. In 2012, he joined the Graduate School of Information Science, Nara Institute of Science and Technology, Nara, Japan, as an Associate Professor. From 2014 to 2015, he was a visiting



a Professor. From 1993 to 2000, he was a Research Associate with Osaka University. From 1999 to 2000, he was Visiting Research Fellow at University of Southampton, Southampton, U.K.. His research interest is wireless communications, including WLAN, WiMAX, CDMA, OFDM, and satellite communications. Dr. Okada is a member of the Institute of Image, Information, and Television Engineers of Japan (ITEJ), the Institute of Television Engineers of Japan, the Institute of Electrical, Information, and Communication Engineers of Japan (IEICE), and the Information Processing Society of Japan (IPSJ). He received the Young Engineer Award from IEICE in 1999.

Minoru Okada received the B.E. degree from the University of Electro-Communications, Tokyo, Japan, in 1990. The M.E and Ph.D. degrees were received from Osaka University, Osaka, Japan, in 1992 and 1998, respectively, all in communications engineering. In 2000, he joined the Graduate School of Information Science, Nara Institute of Science and Technology, Nara, Japan, as an Associate Professor and became



Tomonori Sato received his B.E. degree in communications engineering from Osaka University Osaka Japan in 2008, and his M.E. and Ph.D. degrees from Graduate School of Information Science, Nara Institute of Science and Technology (NAIST) in 2010 and 2013, respectively. His research interest includes the radio sensing and researching intruder detection system using LCX in the school with Okada. His research in-

terests include LCX, signal processing, wireless communication. Now, he works at Hitachi Metals, Ltd.